18 Castagna M, Takai Y, Kaibuchi K, Sano K, Kikkawa U, Nishizuka Y. Direct activation of calcium-activated, phospholipid-dependent protein kinase by tumor-promoting phorbol esters. *J Biol Chem* 1982; **257**: 7847–7851.
19 Ryves WJ, Evans AT, Olivier AR, Parker PJ, Evans FJ. Activation of the PKC-isotypes alpha, beta 1, gamma, delta and epsilon by phorbol esters of different biological activities. *FEBS Lett* 1991; **288**: 5–9.
20 Burden DA, Kingma PS, Froelich-Ammon SJ *et al*. Topoisomerase II etoposide interactions direct the formation of drug-induced enzyme–DNA cleavage complexes. *J Biol Chem* 1996; **271**: 29 238–29 244.
21 Skovronsky DM, Moore DB, Milla ME, Doms RW, Lee VM. Protein kinase C-dependent alpha-secretase competes with beta-secretase for cleavage of amyloid-beta precursor protein in the trans-golgi network. *J Biol Chem* 2000; **275**: 2568–2575.
22 Diaz-Rodriguez E, Montero JC, Esparis-Ogando A, Yuste L, Pandiella A. Extracellular signal-regulated kinase phosphorylates tumor necrosis factor alpha-converting enzyme at threonine 735: A potential role in regulated shedding. *Mol Biol Cell* 2002; **13**: 2031–2044.
23 Robinson MJ, Cobb MH. Mitogen-activated protein kinase pathways. *Curr Opin Cell Biol* 1997; **9**: 180–186.
24 Lanni C, Mazzucchelli M, Porrello E, Govoni S, Racchi M. Differential involvement of protein kinase C alpha and epsilon in the regulated secretion of soluble amyloid precursor protein. *Eur J Biochem* 2004; **271**: 3068–3075.
25 Lee W, Boo JH, Jung MW *et al*. Amyloid beta peptide directly inhibits PKC activation. *Mol Cell Neurosci* 2004; **26**: 222–231.
26 Favit A, Grimaldi M, Nelson TJ, Alkon DL. Alzheimer's-specific effects of soluble beta-amyloid on protein kinase C-alpha and -gamma degradation in human fibroblasts. *Proc Natl Acad Sci USA* 1998; **95**: 5562–5567.
27 Isagawa T, Mukai H, Oishi K *et al*. Dual effects of PKNalpha and protein kinase C on phosphorylation of tau protein by glycogen synthase kinase-3beta. *Biochem Biophys Res Commun* 2000; **273**: 209–212.
28 Crary JF, Shao CY, Mirra SS, Hernandez AI, Sacktor TC. Atypical protein kinase C in neurodegenerative disease I: PKMzeta aggregates with limbic neurofibrillary tangles and AMPA receptors in Alzheimer disease. *J Neuropathol Exp Neurol* 2006; **65**: 319–326.
29 Shao CY, Crary JF, Rao C, Sacktor TC, Mirra SS. Atypical protein kinase C in neurodegenerative disease II: PKCiota/lambda in tauopathies and alpha-synucleinopathies. *J Neuropathol Exp Neurol* 2006; **65**: 327–335.
30 Pardo OE, Wellbrock C, Khanzada UK *et al*. FGF-2 protects small cell lung cancer cells from apoptosis through a complex involving PKCepsilon, B-Raf and S6K2. *EMBO J* 2006; **25**: 3078–3088.
31 Youdim MB, Bar Am O, Yogev-Falach M *et al*. Rasagiline: Neurodegeneration, neuroprotection, and mitochondrial permeability transition. *J Neurosci Res* 2005; **79**: 172–179.
32 Levites Y, Amit T, Mandel S, Youdim MB. Neuroprotection and neurorescue against Abeta toxicity and PKC-dependent release of nonamyloidogenic soluble precursor protein by green tea polyphenol (-)-epigallocatechin-3-gallate. *FASEB J* 2003; **17**: 952–954.
33 Mandel S, Weinreb O, Amit T, Youdim MB. Mechanism of neuroprotective action of the anti-Parkinson drug rasagiline and its derivatives. *Brain Res Brain Res Rev* 2005; **48**: 379–387.
34 Weinreb O, Bar-Am O, Amit T, Chillag-Talmor O, Youdim MB. Neuroprotection via pro-survival protein kinase C isoforms associated with Bcl-2 family members. *FASEB J* 2004; **18**: 1471–1473.
35 Hu Y, Bally M, Dragowska WH, Mayer L. Inhibition of mitogen-activated protein kinase/extracellular signal-regulated kinase kinase enhances chemotherapeutic effects on H460 human non-small cell lung cancer cells through activation of apoptosis. *Mol Cancer Ther* 2003; **2**: 641–649.
36 Mizutani T, Nakashima S, Nozawa Y. Changes in the expression of protein kinase C (PKC), phospholipases C (PLC) and D (PLD) isoforms in spleen, brain and kidney of the aged ratsT-PCR and western blot analysis. *Mech Ageing Dev* 1998; **105**: 151–172.

Neuroscience Letters 487 (2011) 354–357

Contents lists available at ScienceDirect

Neuroscience Letters

journal homepage: www.elsevier.com/locate/neulet

Association between CAG repeat length in the *PPP2R2B* gene and Alzheimer disease in the Japanese population

Ryo Kimura[a,*], Takashi Morihara[b], Takashi Kudo[b], Kouzin Kamino[c], Masatoshi Takeda[b]

[a] Department of Psychiatry, Osaka General Medical Center, 3-1-56 Bandai Higashi, Sumiyoshi-ku, Osaka 558-8558, Japan
[b] Department of Psychiatry, Osaka University Graduate School of Medicine, Osaka, Japan
[c] National Hospital Organization, Shoraiso Hospital, Nara, Japan

ARTICLE INFO

Article history:
Received 24 August 2010
Received in revised form 10 October 2010
Accepted 20 October 2010

Key words:
Alzheimer disease
CAG repeat
PPP2R2B

ABSTRACT

We analyzed the association between *PPP2R2B* gene CAG repeat length and Alzheimer disease (AD) susceptibility in the Japanese population. Blood samples were collected from 218 late-onset AD patients and 86 controls. DNA fragments containing the target CAG repeat region were amplified using polymerase chain reaction (PCR). PCR products were sequenced using ABI PRISM 310 genetic analyzer. The mean CAG repeat length did not differ significantly between the control and AD groups. In contrast, the frequency of CAG repeats shorter than 15 was significantly higher in AD group, specifically in the AD with APOE4 subgroup, than in the control group. The results suggest that CAG repeat lengths in the *PPP2R2B* gene may be potential genetic markers for AD susceptibility in the Japanese population.

Alzheimer disease (AD) is the most common cause of dementia in the elderly, and is characterized by progressive cognitive decline and cerebral atrophy. The primary pathological feature of AD is the presence of neurofibrillary tangles and senile plaques in the brain [26]. The presence of the ε4 allele of the apolipoprotein E (APOE) gene (*APOE4*) confers a heightened risk of late-onset AD in multiple genetic backgrounds [4]. Although trinucleotide repeats are common features of the human genome, the trinucleotide repeat number varies among individuals and the lengths of these repeats is associated with many genetic diseases, including Huntington disease (HD) and Dentatorubral-pallidoluysian atrophy (DRPLA) [25]. A majority of spinocerebellar ataxias (SCAs) are caused by the expansion of trinucleotide repeats. SCAs are a group of autosomal dominant progressive neurodegenerative disorders that are characterized by overlapping and variable phenotypes [20]. Spinocerebellar ataxia type 12 (SCA12) is caused by CAG repeat expansion in the non-coding region of the *PPP2R2B* gene [11]. Clinical symptoms of SCA12 include dementia, upper limb tremor, and extra pyramidal symptoms. Brain magnetic resonance images of the affected individuals revealed cerebral and cerebellar atrophy [11,23].

The *PPP2R2B* gene, which encodes a brain-specific regulatory B subunit of the serine/threonine protein phosphatase 2A (PP2A), is located on chromosome 5q31–33 and is widely expressed in brain neurons [21]. PP2A has been implicated in cell cycle and proliferation and development and regulation of multiple signal transduction pathways [30]. In addition, PP2A dephosphorylates the hyperphosphorylated tau protein [7]. It is suggested that PP2A-mediated dephosphorylation of tau is facilitated by the B regulatory subunit of PP2A [6]. Tau, an axonal microtubule-associated protein, promotes microtubule assembly and stabilization [17], and tau phosphorylation has been implicated, to varying degrees, in AD pathogenesis [12]. Because of the overlap between the SCA12 phenotype and certain aspects of AD, including the functional role of PP2A, it is important to determine the association between the *PPP2R2B* gene and AD. Recently, Chen et al. reported that the presence of short alleles of the CAG repeat in the *PPP2R2B* gene is associated with increased AD susceptibility in the Han Chinese [3]. However, the existence of such an association among other population group is uncertain. In the present study, we investigated the association between *PPP2R2B* gene CAG repeat lengths and AD susceptibility in the Japanese population.

Patients with late-onset AD were diagnosed with definite or probable AD according to the criteria of the National Institute of Neurological and Communicative Disorders and Stroke Alzheimer's Disease and Related Disorders Association [22]. The control group consisted of non-demented elderly subjects from the general population. After written informed consent was obtained, peripheral blood was collected from 218 late-onset AD patients (mean age: 79.0 years; women: 65.6%) and 86 control subjects (mean age: 74.7 years; women: 52.3%). The protocol for specimen collection was approved by the Genome Ethical Committee of Osaka University Graduate School of Medicine.

DNA was extracted from peripheral blood nuclear cells using the phenol–chloroform method or the QIAamp DNA Blood Kit (Qiagen). CAG repeats in the *PPP2R2B* gene were identified

* Corresponding author. Tel.: +81 6 6692 1201; fax: +81 6 6606 7000.
E-mail address: kimura@psy.med.osaka-u.ac.jp (R. Kimura).

0304-3940/$ – see front matter © 2010 Elsevier Ireland Ltd. All rights reserved.
doi:10.1016/j.neulet.2010.10.055

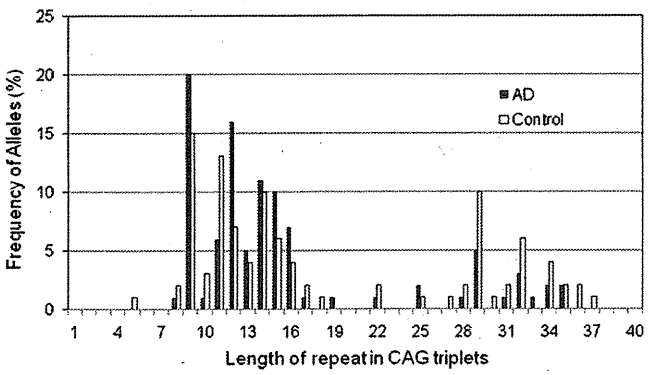

Fig. 1. Distribution of allele frequencies against the CAG repeat numbers in the *PPP2R2B* gene of control subjects and AD patients.

by polymerase chain reaction (PCR) amplification using 6FAM dye-labeled forward (5′-TGCTGGGAAAGAGTCGTG-3′) and reverse (5′-GCCCGCGCACTCACCCTC-3′) primers. The PCR was performed with 36 cycles consisting of two cycles of 30 s at 95 °C and 30 s at 70 °C, two cycles of 30 s at 95 °C and 30 s at 65 °C, two cycles of 30 s at 95 °C and 30 s at 60 °C, and 30 cycles of 30 s at 95 °C, 30 s at 56 °C, and 30 s at 72 °C preceded by 10 min at 95 °C and followed by 10 min at 72 °C. PCR products were electrophoresed in a capillary in an automated ABI PRISM 310 genetic analyzer (Applied Biosystems). Analysis was performed with GenScan analysis software (Applied Biosystems) [11]. The *APOE* genotype was determined using a PCR-RFLP method [15].

Statistical analysis was performed using JMP (version 7.0, SAS Institute, Cary, NC). The 2-sided Mann–Whitney's *U*-test was used to evaluate the difference in CAG repeat distribution between the AD and control groups. The difference in the CAG repeat allele frequencies between the groups was further tested by the Chi-square test. Each value represents mean (standard error). A *p*-value of <0.05 was considered statistically significant.

The frequency distribution of CAG repeat alleles in the *PPP2R2B* genes was analyzed in 218 LOAD patients and 86 controls. In Fig. 1, the CAG repeat number (*X*-axis) is plotted against the frequency of distributions (%) (*Y*-axis). The repeat range was 5–37 and 8–35 in the control and AD groups, respectively. Pathological expansion of CAG repeats was not detected in the AD and control groups. The most common lengths were 9 (15.3%) triplets in the control group. Similarly, in the AD group, the most common lengths were 9 (20.0%) triplets. The mean CAG repeat lengths in the AD and control groups (14.2 and 16.6, respectively) were not statistically different ($p = 0.158$). In addition, when we divided the AD group into APOE4 and non-APOE4 subgroups, we found that the mean CAG repeat lengths of both subgroups (13.9 and 14.5, respectively) were not significantly different from that of the control group (Table 1).

Table 2
Short (≤15) and long (15>) alleles: CAG repeat number in *PPP2R2B*; the short and long allele repeat numbers in the AD and control groups were compared.

Group	Allele number			*p* value	OR
	Total	Short (≤15)	Long (>15)		
Control	172	110 (64%)	62 (36%)		
Control with APOE4	24	16 (67%)	8 (33%)	0.267	
Control without APOE4	148	94 (64%)	54 (36%)	0.022*	1.58
AD	436	320 (73%)	116 (27%)	0.021*	1.55
AD with APOE4	212	163 (77%)	49 (23%)	0.005*	1.87
AD without APOE4	224	157 (70%)	67 (30%)	0.197	

Differences in the allele repeat numbers in the AD and control groups were determined using Chi-square test.
* $p < 0.05$, statistically significant.
OR, odds ratio.

Because the mean CAG repeat length among all subjects was 15, we dichotomized the alleles into short (≤15) and long (15>) categories. Statistical analysis revealed that the frequency of CAG repeats shorter than 15 was significantly higher in the AD group than in the control group ($p = 0.021$, odds ratio = 1.55) (Table 2). Compared to the controls, the AD subgroups, APOE4 and non-APOE4, each had a significantly higher frequency of CAG repeats shorter than 15 ($p = 0.005$, odds ratio = 1.87). However, there was no significant difference in the allele frequency distribution between the non-APOE4 AD group and the control group ($p = 0.197$) (Table 2). Additionally, a comparison of the allele frequency distributions of the control subgroups, APOE4 and non-APOE4 with that of the AD revealed that the frequency of CAG repeats shorter than 15 was significantly higher in the AD groups than in the control without APOE4 groups ($p = 0.022$, odds ratio = 1.58) (Table 2).

SCA12 is a relatively rare late-onset neurodegenerative disorder characterized by diffuse cerebral and cerebellar atrophy [11]. The phenotype typically involves action tremor of upper extremities and various symptoms, including dementia. SCA12 is caused by CAG repeat expansion in the non-coding region of the *PPP2R2B* gene [10,11]. Pathogenic CAG repeat expansions have been detected in SCA12 patients in the range of 55–69 to 66–78, but normal individuals from different ethnic populations have exhibited ranges from 7–28 to 9–45 [2,3,5,11,27–29]. A correlation between the SCA12 phenotype and certain aspects of AD has been suggested. However, the lone study that analyzed the association between CAG repeat expansions in the *PPP2R2B* gene and AD susceptibility reported that the frequency of the Han Chinese individuals carrying the short 5-, 6-, and 7-triplet alleles was notably higher in AD patients [3].

In the present study, we investigated the length of *PPP2R2B* gene CAG repeats in AD patients and control subjects in the Japanese population. The mean CAG repeat lengths in the AD and control groups were not statistically different. In contrast, we found that the frequency of CAG repeats shorter than 15 was significantly higher in the AD group, specifically the AD with APOE4 subgroup

Table 1
Comparison of CAG repeat numbers in control subjects and AD patients.

Group	Control			AD		
	Total	APOE4 (+)	APOE4 (−)	Total	APOE4 (+)	APOE4 (−)
Number	86	12	74	218	106	112
Allele range	5–37	9–34	5–37	8–35	8–35	8–35
Allele with maximum frequency						
Allele	9	9	9	9	9	9
Frequency (%)	15.3	14.2	16.7	20.0	20.1	17.5
Mean (SE)	16.6 (0.8)	14.4 (1.8)	16.9 (0.8)	14.2 (0.5)	13.9 (0.6)	14.5 (0.7)
p value		0.942	0.114	0.158	0.110	0.362

The differences between the CAG repeat numbers in the control and AD groups were assayed using Mann–Whitney's *U*-test.
SE: standard error of the mean.

than in the control group (Table 2). Our results suggested that AD is associated with a lower number of CAG repeats in the *PPP2R2B* gene. This was similar to the findings of a previous report by Chen et al. [3]. However, in our AD patients, we did not find short 5–7 triplet alleles which detected in AD patients in the Han Chinese population. This discrepancy may reflect a genetic differentiation between the Han Chinese and Japanese populations.

The presence of the ε4 allele of *APOE* gene confers a heightened risk of late-onset AD [4]. As compared to individuals without the ε4 alleles, the risk for AD is 2- to 3-fold and about 12-fold higher in individuals carrying one and two ε4 alleles, respectively [1,14,24]. Though several studies have attempted to elucidate the mechanism for this increased risk, how APOE4 influences AD progression has yet to be proven. In particular, we found that the frequency of short CAG repeats (≤15) was higher in the AD with APOE4 group than in the control group. Therefore, it is likely that a short number of CAG repeats of *PPP2R2B* gene play an important role for the progression of late-onset AD with APOE4.

PP2A is composed of three subunits: a catalytic subunit (C), a scaffolding subunit (A), and a regulatory subunit (B). Assembly of the complex with the regulatory B subunit is required for the specificity and regulation of PP2A [31]. In addition, PP2A is the major tau phosphatase that dephosphorylates tau at multiple sites, and its activity is decreased by 30% in the frontal or temporal cortex of AD patients compared to controls [8,18]. This down-regulation of PP2A activity in AD brains is thought to be partially responsible for abnormal tau phosphorylation. Therefore, differences in the CAG repeat lengths in the *PPP2R2B* gene may regulate PP2A activity, leading to AD progression. Through a reporter assay, the short 5–7 triplet alleles were shown to be associated with decreased PPP2R2B promoter activities [3]. However, it has not yet been demonstrated that the short CAG repeat lengths in the PPP2R2B affect PP2A function directly.

APOE plays an important role in the distribution and metabolism of cholesterol in the human body [19]. APOE4 has also been associated with tau hyperphosphorylation in several animal models [9]. In particular, high cholesterol such as in Niemann-Pick C disease might be involved in decreasing membrane fluidity [16]. Therefore, it was recently supposed that signal transduction through the interaction of APOE4 with the neuronal cell membrane might involve AD progression through various kinases and phosphatases [13].

In conclusion, our results suggest that CAG repeat lengths in the *PPP2R2B* gene may be potential genetic markers for AD susceptibility in the Japanese population. Further investigations are required to confirm the role of the *PPP2R2B* gene in AD using a larger sample size and a different population group.

Conflicts of interest

None of the authors has any conflicts of interest.

Acknowledgements

We thank Drs. E. Kamagata, H. Tanimukai, and H. Matusnaga for useful suggestions and M. Yamamoto for excellent technical assistance. This work was funded by the Future Program and the Japan Society for the Promotion of Science (JSPS), and by a Grant-in-Aid for Scientific Research on Priority Areas "Applied Genomics" from the Ministry of Education, Culture, Sports, Science and Technology of Japan.

References

[1] L. Bertram, M.B. McQueen, K. Mullin, D. Blacker, R.E. Tanzi, Systematic meta-analyses of Alzheimer disease genetic association studies: the AlzGene database, Nat. Genet. 39 (2007) 17–23.
[2] A. Brusco, C. Cagnoli, A. Franco, E. Dragone, A. Nardacchione, E. Grosso, P. Mortara, R. Mutani, N. Migone, L. Orsi, Analysis of SCA8 and SCA12 loci in 134 Italian ataxic patients negative for SCA1-3, 6 and 7 CAG expansions, J. Neurol. 249 (2002) 923–929.
[3] C.M. Chen, Y.T. Hou, J.Y. Liu, Y.R. Wu, C.H. Lin, H.C. Fung, W.C. Hsu, Y. Hsu, S.H. Lee, H.M. Hsieh-Li, M.T. Su, S.T. Chen, H.Y. Lane, G.J. Lee-Chen, PPP2R2B CAG repeat length in the Han Chinese in Taiwan: association analyses in neurological and psychiatric disorders and potential functional implications, Am. J. Med. Genet. B: Neuropsychiatr. Genet. 150B (2009) 124–129.
[4] E.H. Corder, A.M. Saunders, W.J. Strittmatter, D.E. Schmechel, P.C. Gaskell, G.W. Small, A.D. Roses, J.L. Haines, M.A. Pericak-Vance, Gene dose of apolipoprotein E type 4 allele and the risk of Alzheimer's disease in late onset families, Science 261 (1993) 921–923.
[5] H. Fujigasaki, I.C. Verma, A. Camuzat, R.L. Margolis, C. Zander, A.S. Lebre, L. Jamot, R. Saxena, I. Anand, S.E. Holmes, C.A. Ross, A. Durr, A. Brice, SCA12 is a rare locus for autosomal dominant cerebellar ataxia: a study of an Indian family, Ann. Neurol. 49 (2001) 117–121.
[6] C.X. Gong, I. Grundke-Iqbal, K. Iqbal, Dephosphorylation of Alzheimer's disease abnormally phosphorylated tau by protein phosphatase-2A, Neuroscience 61 (1994) 765–772.
[7] C.X. Gong, T. Lidsky, J. Wegiel, L. Zuck, I. Grundke-Iqbal, K. Iqbal, Phosphorylation of microtubule-associated protein tau is regulated by protein phosphatase 2A in mammalian brain. Implications for neurofibrillary degeneration in Alzheimer's disease, J. Biol. Chem. 275 (2000) 5535–5544.
[8] C.X. Gong, S. Shaikh, J.Z. Wang, T. Zaidi, I. Grundke-Iqbal, K. Iqbal, Phosphatase activity toward abnormally phosphorylated tau: decrease in Alzheimer disease brain, J. Neurochem. 65 (1995) 732–738.
[9] F.M. Harris, W.J. Brecht, Q. Xu, R.W. Mahley, Y. Huang, Increased tau phosphorylation in apolipoprotein E4 transgenic mice is associated with activation of extracellular signal-regulated kinase: modulation by zinc, J. Biol. Chem. 279 (2004) 44795–44801.
[10] S.E. Holmes, E.O. Hearn, C.A. Ross, R.L. Margolis, SCA12: an unusual mutation leads to an unusual spinocerebellar ataxia, Brain Res. Bull. 56 (2001) 397–403.
[11] S.E. Holmes, E.E. O'Hearn, M.G. McInnis, D.A. Gorelick-Feldman, J.J. Kleiderlein, C. Callahan, N.G. Kwak, R.G. Ingersoll-Ashworth, M. Sherr, A.J. Sumner, A.H. Sharp, U. Ananth, W.K. Seltzer, M.A. Boss, A.M. Vieria-Saecker, J.T. Epplen, O. Riess, C.A. Ross, R.L. Margolis, Expansion of a novel CAG trinucleotide repeat in the 5′ region of PPP2R2B is associated with SCA12, Nat. Genet. 23 (1999) 391–392.
[12] K. Iqbal, C. Alonso Adel, S. Chen, M.O. Chohan, E. El-Akkad, C.X. Gong, S. Khatoon, B. Li, F. Liu, A. Rahman, H. Tanimukai, I. Grundke-Iqbal, Tau pathology in Alzheimer disease and other tauopathies, Biochim. Biophys. Acta 1739 (2005) 198–210.
[13] K. Iqbal, F. Liu, C.X. Gong, C. Alonso Adel, I. Grundke-Iqbal, Mechanisms of tau-induced neurodegeneration, Acta Neuropathol. 118 (2009) 53–69.
[14] J. Kim, J.M. Basak, D.M. Holtzman, The role of apolipoprotein E in Alzheimer's disease, Neuron 63 (2009) 287–303.
[15] R. Kimura, K. Kamino, M. Yamamoto, A. Nuripa, T. Kida, H. Kazui, R. Hashimoto, T. Tanaka, T. Kudo, H. Yamagata, Y. Tabara, T. Miki, H. Akatsu, K. Kosaka, E. Funakoshi, K. Nishitomi, G. Sakaguchi, A. Kato, H. Hattori, T. Uema, M. Takeda, The DYRK1A gene, encoded in chromosome 21 Down syndrome critical region, bridges between beta-amyloid production and tau phosphorylation in Alzheimer disease, Hum. Mol. Genet. 16 (2007) 15–23.
[16] Z Korade, A.K. Kenworthy, Lipid rafts, cholesterol, and the brain, Neuropharmacology 55 (2008) 1265–1273.
[17] V.M. Lee, M. Goedert, J.Q. Trojanowski, Neurodegenerative tauopathies, Annu. Rev. Neurosci. 24 (2001) 1121–1159.
[18] F. Liu, I. Grundke-Iqbal, K. Iqbal, C.X. Gong, Contributions of protein phosphatases PP1, PP2A, PP2B and PP5 to the regulation of tau phosphorylation, Eur. J. Neurosci. 22 (2005) 1942–1950.
[19] R.W. Mahley, B.P. Nathan, R.E. Pitas, E. Apolipoprotein, Structure, function, and possible roles in Alzheimer's disease, Ann. N. Y. Acad. Sci. 777 (1996) 139–145.
[20] M.U Manto, The wide spectrum of spinocerebellar ataxias (SCAs), Cerebellum 4 (2005) 2–6.
[21] R.E. Mayer, P. Hendrix, P. Cron, R. Matthies, S.R. Stone, J. Goris, W. Merlevede, J. Hofsteenge, B.A. Hemmings, Structure of the 55-kDa regulatory subunit of protein phosphatase 2A: evidence for a neuronal-specific isoform, Biochemistry 30 (1991) 3589–3597.
[22] G. McKhann, D. Drachman, M. Folstein, R. Katzman, D. Price, E.M. Stadlan, Clinical diagnosis of Alzheimer's disease: report of the NINCDS-ADRDA Work Group under the auspices of Department of Health and Human Services Task Force on Alzheimer's Disease, Neurology 34 (1984) 939–944.
[23] E. O'Hearn, S.E. Holmes, P.C. Calvert, C.A. Ross, R.L. Margolis, SCA-12: tremor with cerebellar and cortical atrophy is associated with a CAG repeat expansion, Neurology 56 (2001) 299–303.
[24] A.D. Roses, Apolipoprotein E alleles as risk factors in Alzheimer's disease, Annu. Rev. Med. 47 (1996) 387–400.
[25] C.A. Ross, Polyglutamine pathogenesis: emergence of unifying mechanisms for Huntington's disease and related disorders, Neuron 35 (2002) 819–822.
[26] D.J. Selkoe, Alzheimer's disease is a synaptic failure, Science 298 (2002) 789–791.
[27] A.K. Srivastava, S. Choudhry, M.S. Gopinath, S. Roy, M. Tripathi, S.K. Brahmachari, S. Jain, Molecular and clinical correlation in five Indian families with spinocerebellar ataxia 12, Ann. Neurol. 50 (2001) 796–800.

[28] A. Sulek, D. Hoffman-Zacharska, M. Bednarska-Makaruk, W. Szirkowiec, J. Zaremba, Polymorphism of trinucleotide repeats in non-translated regions of SCA8 and SCA12 genes: allele distribution in a Polish control group, J. Appl. Genet. 45 (2004) 101–105.
[29] H.F. Tsai, C.S. Liu, T.M. Leu, F.C. Wen, S.J. Lin, C.C. Liu, D.K. Yang, C. Li, M. Hsieh, Analysis of trinucleotide repeats in different SCA loci in spinocerebellar ataxia patients and in normal population of Taiwan, Acta Neurol. Scand. 109 (2004) 355–360.
[30] D.M. Virshup, Protein phosphatase 2A: a panoply of enzymes, Curr. Opin. Cell. Biol. 12 (2000) 180–185.
[31] Y. Xu, Y. Chen, P. Zhang, P.D. Jeffrey, Y. Shi, Structure of a protein phosphatase 2A holoenzyme: insights into B55-mediated Tau dephosphorylation, Mol. Cell 31 (2008) 873–885.

EXTRA
Dementia
and Geriatric
Cognitive Disorders

Dement Geriatr Cogn Disord Extra 2011;1:20–30
DOI: 10.1159/000323561
Published online: January 6, 2011

Original Research Article

Different Characteristics of Cognitive Impairment in Elderly Schizophrenia and Alzheimer's Disease in the Mild Cognitive Impairment Stage

Hiroaki Kazui[a] Tetsuhiko Yoshida[a, b] Masahiko Takaya[a] Hiromichi Sugiyama[a] Daisuke Yamamoto[a] Yumiko Kito[a, c] Tamiki Wada[a] Keiko Nomura[a] Yuka Yasuda[a] Hidenaga Yamamori[a] Kazutaka Ohi[a] Motoyuki Fukumoto[a] Naomi Iike[a] Masao Iwase[a] Takashi Morihara[a] Shinji Tagami[a] Eku Shimosegawa[d] Jun Hatazawa[d] Yoshiyuki Ikeda[e] Eiichi Uchida[e] Toshihisa Tanaka[a] Takashi Kudo[a] Ryota Hashimoto[a, f] Masatoshi Takeda[a]

[a]Psychiatry, Department of Integrated Medicine, Division of Internal Medicine, Osaka University Graduate School of Medicine, [b]Department of Psychiatry, National Hospital Organization Osaka National Hospital, [c]Department of Psychiatry, Nissay Hospital, [d]Department of Nuclear Medicine and Tracer Kinetics, Osaka University Graduate School of Medicine, [e]Department of Radiology, Uchida Clinic, and [f]Molecular Research Center for Children's Mental Development, United Graduate School of Child Development, Osaka University, Kanazawa University and Hamamatsu University School of Medicine, Osaka, Japan

Key Words
Alzheimer's disease · Attention deficit · Delayed recall · Executive function · Recent memory · Three-dimensional stereotactic surface projections · Voxel-based specific region analysis · Working memory

Abstract
We compared indices of the revised version of the Wechsler Memory Scale (WMS-R) and scaled scores of the five subtests of the revised version of the Wechsler Adult Intelligence Scale (WAIS-R) in 30 elderly schizophrenia (ES) patients and 25 Alzheimer's disease (AD) patients in the amnestic mild cognitive impairment (aMCI) stage (AD-aMCI). In the WMS-R, attention/concentration was rated lower and delayed recall was rated higher in ES than in AD-aMCI, although general memory was comparable in the two groups. In WAIS-R, digit symbol substitution, similarity, picture completion, and block design scores were significantly lower in ES than in AD-aMCI, but the information scores were comparable between the two groups. Delayed recall and

Hiroaki Kazui, MD, PhD

Psychiatry, Department of Integrated Medicine, Division of Internal Medicine
Osaka University Graduate School of Medicine, D3 2-2 Yamadaoka, Suita-City
Osaka 565-0871 (Japan)
Tel. +81 66 879 3051, Fax +81 66 879 3059, E-Mail kazui@psy.med.osaka-u.ac.jp

EXTRA
Dementia
and Geriatric
Cognitive Disorders

Dement Geriatr Cogn Disord Extra 2011;1:20–30
DOI: 10.1159/000323561
Published online: January 6, 2011

forgetfulness were less impaired, and attention, working memory and executive function were more impaired in ES than in AD-aMCI. These results should help clinicians to distinguish ES combined with AD-aMCI from ES alone.

Introduction

Schizophrenia is a common psychiatric disease with onset usually occurring during adolescence or early adulthood. Recently, new atypical antipsychotic drugs for schizophrenia have been developed, and social systems to support schizophrenia patients have been established. As a result, schizophrenia patients are now living longer than they used to [1], and the number of elderly schizophrenia (ES) patients is increasing. The number of Alzheimer's disease (AD) patients has also increased due to the rapid aging of society. Although the incidence of AD rises with age, AD also occurs in younger patients; the prevalence rate of AD in people aged ≤64 years is 0.12 cases per 1,000 people (http://www.mhlw.go.jp/houdou/2009/03/h0319–2.html; Japanese Ministry of Health, Labor and Welfare). Therefore, there are many ES patients who also have AD, and their number is supposed to be increasing. In clinical settings, there is a growing need to differentiate between age-related and AD-related cognitive impairment in patients who have developed schizophrenia in adolescence or middle age.

Because some clinical characteristics of schizophrenia and AD are similar, differentiation between ES and AD can be difficult. Neuropsychiatric symptoms, such as apathy, poverty of speech, and delusional thinking, are common in both types of patients. Neuroimaging studies have shown volume loss in the hippocampus [2] and in the frontal lobe [3] in schizophrenia, and similar losses have been observed in AD [4]. Furthermore, patients with schizophrenia are impaired in various domains of cognition, such as memory, working memory, and executive function [5]. These symptoms are also observed in patients with AD.

Acetylcholine esterase inhibitors have been developed for the treatment of AD. Although administration of these agents does not result in a radical improvement of symptoms, their early administration can improve the prognosis of AD patients [6]. In addition, disease-modifying drugs for AD are now being developed. Thus, early diagnosis and early initiation of treatment are important in AD patients. One method to identify early AD with a high probability is the measurement of amnestic mild cognitive impairment (aMCI), which is a syndrome characterized by memory performance below the age norm, while intellectual functioning and activities of daily living are otherwise unimpaired [7]. A substantial proportion of patients with aMCI later develop clinically diagnosable AD [7]. In order to treat early-stage ES patients who have AD in the aMCI stage (AD-aMCI) for AD, it is necessary to differentiate between ES combined with AD, and ES alone. As a first step toward this goal, in this study, we clarified the degree of cognitive impairment in patients with ES compared to patients with AD-aMCI.

Methods

Subjects

All patients in this study were recruited from the Department of Neuropsychiatry of the Osaka University Medical Hospital, which includes Schizophrenia and Neuropsychological Clinics. At both clinics, patients underwent standard neuropsychological examinations as well as routine laboratory tests and cranial magnetic resonance imaging (MRI). Single pho-

Dement Geriatr Cogn Disord Extra 2011;1:20–30
DOI: 10.1159/000323561
Published online: January 6, 2011

Table 1. Comparison of characteristics of the ES and AD-aMCI groups with and without WAIS-R

Characteristics	ES group			AD-aMCI group		
	with WAIS-R	without WAIS-R	p value	with WAIS-R	without WAIS-R	p value
Sex, male/female	5/9	10/6	0.14	7/6	7/5	0.57
Age, years	56.6 ± 5.5	57.1 ± 5.7	0.79	72.6 ± 6.0	70.2 ± 9.5	0.44
Education, years	13.1 ± 2.6	13.3 ± 2.2	0.79	13.7 ± 3.3	13.4 ± 1.8	0.8
MMSE total score	–	–	–	26.1 ± 1.9	27.0 ± 2.1	0.27
WMS-R GM index	81.3 ± 15.5	79.1 ± 17.0	0.75	80.5 ± 13.1	74.9 ± 6.1	0.19
WMS-R AC index	84.8 ± 10.3	94.8 ± 16.0	0.09	99.8 ± 11.1	97.3 ± 12.7	0.59
WMS-R DR index	75.9 ± 15.9	76.6 ± 18.4	0.92	61.5 ± 9.7	55.8 ± 6.5	0.1

ton emission computed tomography (SPECT) was performed on patients with aMCI at the Neuropsychological Clinic. The clinical and investigative data were collected in a standardized manner and were entered into each registry. In this study, we selected patients with ES and patients with AD-aMCI who met the inclusion criteria mentioned below for each group from the registry. In the Schizophrenia Clinic, we began using the revised version of the Wechsler Adult Intelligence Scale (WAIS-R) in March 2004 and then switched to the third version of the WAIS (WAIS-III) in October 2006. In the Neuropsychological Clinic, we began using five subtests of the WAIS-R in September 2002 and switched to five subtests of the WAIS-III in February 2009. In this study, we selected patients who were evaluated with the WAIS-R, because few patients with AD-aMCI were evaluated with the WAIS-III and then followed up until they reached the dementia stage. The revised version of the Wechsler Memory Scale (WMS-R) has been used in both clinics as a memory test because the third version of the WMS (WMS-III) is not standardized and cannot be used in Japan. In both clinics, the WMS-R was usually used before the WAIS-R. However, in some cases, there was no opportunity to use the WAIS-R.

ES Group

Thirty patients with schizophrenia (15 women and 15 men) were selected from the Schizophrenia Clinic registry. The mean age of the patients was 56.9 ± 5.5 years, and the mean years of education were 13.2 ± 2.3. All subjects in the ES group (1) met the criteria for schizophrenia based on the Structured Clinical Interview of the Diagnostic and Statistical Manual of Mental Disorders, 4th ed., Text Revision (DSM-IV-TR); (2) were aged ≥50 years [8]; (3) showed first symptoms of schizophrenia before 65 years of age; (4) had been evaluated by either the WMS-R or the WAIS-R; (5) had no other neurological disease, and (6) had no evidence of focal brain lesions on MRI. Of the 30 patients, 14 were given the WAIS-R (group with WAIS-R) and the other 16 were not given the WAIS-R (group without WAIS-R). There were no significant differences in gender, age, education, or WMS-R indices between the ES groups with and without WAIS-R (table 1). Other demographic data on the ES group are summarized in table 2. Mean duration of hospitalization was short, although mean duration of disease was long. Many patients received atypical antipsychotic drugs at the time of neuropsychological assessment in this study. There were no significant differences between the groups with and without WAIS-R in any of the items except for the positive/negative symptom scores of the Positive and Negative Syndrome Scale (PANSS). Both PANSS scores were higher in the group without WAIS-R than in the group with WAIS-R. Four of the 30 patients with ES were not given the WMS-R.

Dement Geriatr Cogn Disord Extra 2011;1:20–30
DOI: 10.1159/000323561
Published online: January 6, 2011

Table 2. Characteristics of the ES group

Characteristics	ES with WAIS-R mean ± SD	ES without WAIS-R mean ± SD	p value	Total mean ± SD (range)
Age of disease onset, years	32.3 ± 12.0	30.1 ± 12.3	0.64	31.1 ± 12.0 (19.0–61.0)
Duration of untreated psychosis, years	3.6 ± 6.5	4.1 ± 8.4	0.87	3.9 ± 7.5 (0–26)
Duration of disease, years	23.8 ± 11.7	27.4 ± 10.7	0.41	25.8 ± 11.1 (1–45)
Total duration of hospitalization, months	14.0 ± 12.2	9.7 ± 19.6	0.56	11.4 ± 16.8 (0–72)
Daily dose of antipsychotic drugs (chlorpromazine equivalent), mg	554.7 ± 283.6	469.1 ± 387.6	0.5	509.0 ± 340.0 (0.0–1,300.0)
Daily dose of atypical antipsychotic drugs (chlorpromazine equivalent), mg	485.7 ± 306.6	318.8 ± 379.9	0.2	396.7 ± 352.0 (0.0–1,300.0)
PANSS score				
Positive symptoms	12.3 ± 4.6	16.3 ± 4.4	0.03	14.5 ± 4.8 (5–28)
Negative symptoms	12.3 ± 3.2	18.3 ± 6.5	0.01	15.5 ± 6.0 (7–30)
Overall severity in the Drug-Induced Extra-Pyramidal Symptoms Scale (n = 21)	0.90 ± 1.9	0.86 ± 0.7	0.94	0.88 ± 1.3 (0–6)

AD-aMCI Group

Twenty-five AD-aMCI patients were selected from the Neuropsychological Clinic registry. The number of males exceeded the number of females (14 males and 11 females). The mean age of the patients was 71.4 ± 7.8 years, the mean years of education were 13.6 ± 2.6, and the mean MMSE score was 26.5 ± 2.0. All subjects in the AD-aMCI group met the criteria for aMCI, which included (1) a memory complaint documented by the patient or another source; (2) a score in the story A recall task in the logical memory II subtest of WMS-R which is less than the age-corrected and education-corrected cutoff score; (3) a score of ≥24 on the MMSE; (4) a total Clinical Dementia Rating (CDR) score of 0.5 and a memory CDR score >0; (5) normal basic and instrumental activities of daily living evaluated with Lawton's Physical Self-Maintenance Scale and Instrumental Activities of Daily Living Scale [9], and (6) no symptoms of dementia based on a clinical examination and an extensive interview with a knowledgeable informant. All subjects in this group also (7) had been evaluated by either the WMS-R or the short form of the Japanese version of the WAIS-R, (8) had no other neurological disease, and (9) had no evidence of focal brain lesions on MRI. To confirm that the aMCI patients had AD in the preclinical stage, at least one of the following three criteria had to be fulfilled: (1) atrophy in the entorhinal cortex on MRI, (2) hypoperfusion in the posterior cingulate cortex (PCC) and precuneus on SPECT, or (3) progression to AD during annual follow-ups. Progression to AD was defined as meeting the criteria of the National Institute of Neurological Disease and Stroke/Alzheimer's Disease and Related Disorders Association (NINCDS-ADRDA) for probable AD and a total CDR score of ≥1.0.

Progression to AD from aMCI during the subsequent follow-ups (up to 8 years) was confirmed in 17 of the 25 patients. Nineteen of the 25 AD-aMCI patients received three-dimensional spoiled gradient echo MRI, which identified atrophy in the entorhinal cortex in 13 of the 19 patients. Twenty-three of the 25 AD-aMCI patients received N-isopropyl-p-[^{123}I]-iodoamphetamine (^{123}I-IMP)-SPECT, and hypoperfusion in either the PCC or precuneus was identified in 12 of the 23 AD-aMCI patients. One patient was recruited due to abnormality on the MRI and 7 patients were recruited due to abnormality on SPECT. Of the 25 patients, 13 were given the five subtests of the WAIS-R (group with WAIS-R) but the other 12 were not (group without WAIS-R). There were no significant differences in gender, age, education,

Dement Geriatr Cogn Disord Extra 2011;1:20–30
DOI: 10.1159/000323561
Published online: January 6, 2011

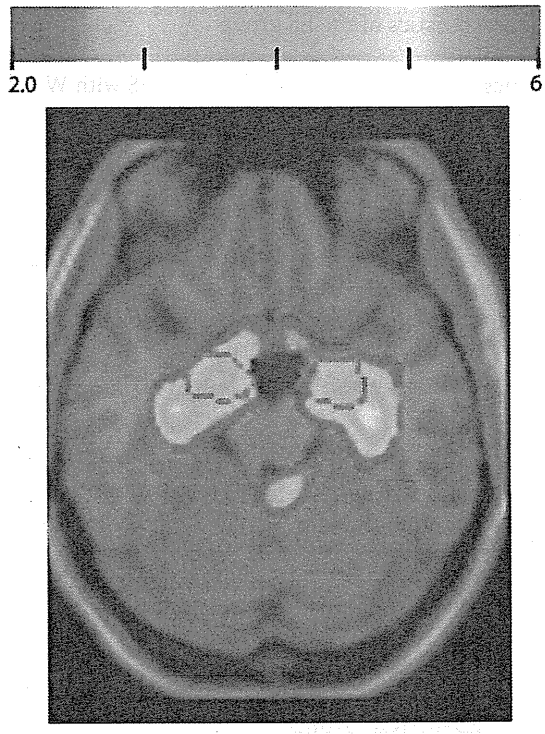

Fig. 1. Z-score map overlaid on an MRI template of a representative patient with AD-aMCI made with VSRAD. This patient was included in the study because of the presence of significant atrophy in the entorhinal cortices on MRI. Parts of the colored areas are in the areas circumscribed by purple lines, indicating significant atrophy in the entorhinal cortices. Purple lines indicate the bilateral entorhinal cortices. Colored areas on MRI are those with a Z-score >2 (significant atrophy). Color bar indicates Z-score.

MMSE score or WMS-R indices between the two groups with and without WAIS-R (table 1). All AD-aMCI patients were administered the WMS-R.

Comparison of Demographic Data in the ES and the AD-aMCI Groups

There was no significant difference between the ES and the AD-aMCI groups in terms of sex ($p = 0.48$, χ^2 test) or education ($p = 0.71$, t test). However, the ES group was significantly younger than the AD-aMCI group ($p < 0.001$, t test).

MRI and SPECT Criteria for the AD-aMCI Group

MRI was performed on a 1.5-tesla system (Signa Excite HD 12x; General Electric Medical Systems, Milwaukee, Wisc., USA). A three-dimensional volumetric acquisition of a T1-weighted gradient echo sequence produced a gapless series of thin sagittal sections that covered the whole calvarium. The operating parameters were as follows: field of view = 240 mm, matrix = 256×256, 124×1.40 mm contiguous sections, TR = 12.55 ms, TE = 4.20 ms, and flip angle = 15°. The three-dimensional T1-weighted MRI data of the patients were analyzed with the voxel-based specific region analysis for AD (VSRAD) [10] (fig. 1). VSRAD contained the MRI data of normal control subjects with a wide age range and could automatically compare the gray matter intensities of the MRI data on a voxel-by-voxel basis between an aMCI patient and age-comparable normal control subjects after a series of steps including segmentation, anatomical standardization and smoothing using Statistical Parametric Mapping 2002 (SPM2; Wellcome Department of Imaging Neuroscience, London, UK). The Z-score is calculated on a voxel-by-voxel basis as (Is – Ic)/SD where Is and Ic are the gray matter intensities of an aMCI patient and the mean of normal control subjects, respectively, and SD is the standard deviation of the gray matter intensities of the normal control subjects. The region of interest was set to the entorhinal cortex in the VSRAD software. Atrophy corresponding to a Z-score >2.0 in the entorhinal cortex was used as a criterion for AD in the VSRAD method.

Dement Geriatr Cogn Disord Extra 2011;1:20–30
DOI: 10.1159/000323561
Published online: January 6, 2011

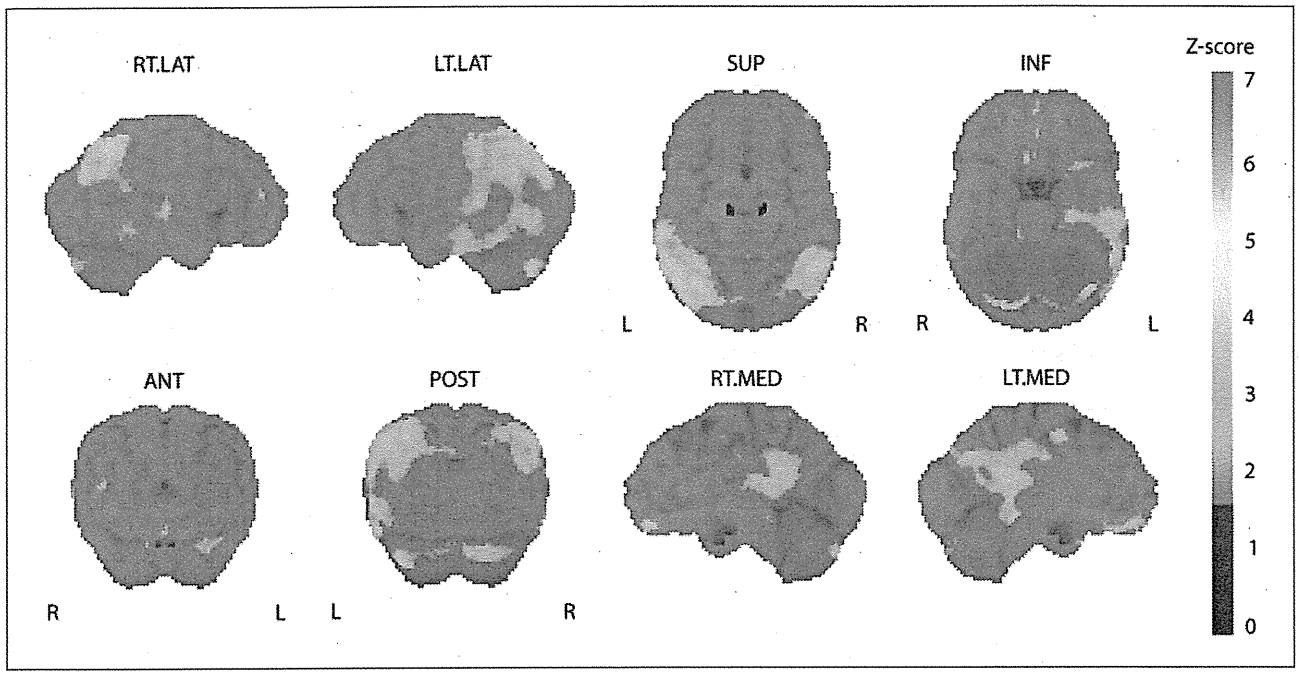

Fig. 2. Z-score map of a representative patient with AD-aMCI made with 3D-SSP. This patient was included in the study because of the presence of hypoperfusion in the PCC and precuneus on SPECT. Colored areas contain PCC and precuneus. Colored areas with significant rCBF reduction with a Z-score of >2.32 were overlaid on original surface images from eight views. Color bar indicates Z-score. RT.LAT = Right lateral; LT.LAT = left lateral; SUP = superior; INF = inferior; ANT = anterior; POST = posterior; RT.MED = right medial; LT.MED = left medial.

^{123}I-IMP-SPECT was performed with a SPECT scanner (SPECT-2000H; Hitachi Medical Co., Tokyo, Japan) and a four-head rotating gamma camera. SPECT data were analyzed using three-dimensional stereotactic surface projection (3D-SSP) software [11] (fig. 2). 3D-SSP contained ^{123}I-IMP-SPECT data of normal control subjects with a wide age range and could automatically compare the regional cerebral blood flow (rCBF) between an aMCI patient and age-comparable normal control subjects. The peak cortical values of the SPECT data were projected back and assigned to the original surface images from eight views on a pixel-by-pixel basis. Z-score was calculated on a pixel-by-pixel basis as (Is – Ic)/SD where Is and Ic are the rCBFs of an aMCI patient and the mean of normal control subjects, respectively, and SD is the standard deviation of the rCBF of the normal control subjects. Areas with a Z-score >2.32 (the significance level of the Z-score) were overlaid on original surface images from eight views. With the computer program Stereotactic Extraction Estimation (SEE) we determined which gyri included the regions with a Z-score >2.32 [12]. In SEE, the percentage of areas with a Z-score >2.32 in each gyrus was calculated and the percentage was called the 'extent'. The presence of areas of hypoperfusion, in which both the Z-score was >2.32 and the extent was >10% [13] in either the PCC or precuneus, was used as the inclusion criteria for AD in the aMCI stage.

Assessment of Cognitive Functions

The attention/concentration (AC) index in the WMS-R was used for measuring attention and working memory, the general memory (GM) index was used for recent memory, and the delayed recall (DR) index for delayed memory. For each index, the normal range is

Dement Geriatr Cogn Disord Extra 2011;1:20–30
DOI: 10.1159/000323561
Published online: January 6, 2011

Table 3. Cognitive impairment in ES and AD-aMC patients

Test/subtest	ES group	AD-aMCI group	p value
WMS-R			
GM index	80.0 ± 16.2	77.8 ± 10.5	0.58
AC index	91.0 ± 14.7	98.6 ± 11.7	0.046
DR index	76.3 ± 17.2	58.8 ± 8.6	<0.001
GM-DR	3.6 ± 10.7	19.9 ± 8.6	<0.001
WAIS-R			
Information	10.1 ± 3.7	11.2 ± 2.8	0.37
Digit symbol substitution	8.0 ± 2.7	11.6 ± 2.3	<0.001
Similarity	9.9 ± 3.2	12.5 ± 2.2	0.024
Picture completion	8.5 ± 4.0	11.2 ± 1.8	0.037
Block design	8.4 ± 2.7	11.5 ± 1.9	0.0018

between 80 and 120 and the mean index of normal subjects is 100. We also defined a new index equal to the GM index minus the DR index (GM-DR), which is a measure of the degree of forgetfulness.

For the WAIS-R, five test data were used in this study. Four of the five subtests were information, digit symbol substitution, similarities, and picture completion, which were selected according to the manual of the short form of the Japanese version of the WAIS-R [14]. Another was a block design to evaluate visuoconstructive function directly, as this dysfunction is a common symptom in AD patients. In each age-corrected score of the subtest, the normal range is between 7 and 13 and the mean score of normal subjects is 10.

Statistical Analyses

Age-corrected scores of both the WMS-R and the five subtests of the WAIS-R were compared between the two groups using a t test. The significance level was set at $p < 0.05$.

Results

Results of the WMS-R

In this study, the mean GM indices in the two groups were around the lower limit of the normal range, and the mean AC indices in ES and AD-aMCI were normal (table 3). The mean DR index of ES was slightly below the normal range, but the mean DR index of AD-aMCI appeared to be significantly lower. The GM indices of the two groups were comparable. The AC index was significantly lower and the DR index was significantly higher in ES than in AD-aMCI. The difference in the GM and DR scores (GM-DR), which is a measure of the degree of forgetfulness, was significantly lower in ES than in AD-aMCI.

Results of the Five Subtests of the WAIS-R

The mean scores of all the subtests of the WAIS-R in this study in both groups were within the normal range (table 3). The information scores of the two groups were comparable, but scores of the digit symbol substitution, similarity, picture completion, and block design subtests were significantly lower in ES than in AD-aMCI.

Dement Geriatr Cogn Disord Extra 2011;1:20–30
DOI: 10.1159/000323561
Published online: January 6, 2011

Discussion

We could not confirm that all AD-aMCI patients in this study developed AD to the dementia stage. However, we were able to select aMCI patients that had AD-specific findings on MRI or SPECT in this study. Pathological abnormalities related to AD, neurofibrillary tangles and neuronal loss, were found to be present in the entorhinal cortex of AD in aMCI stage [15], leading to atrophy in the region on MRI [16]. Because the entorhinal cortex is functionally connected to the PCC [17], the reduction of rCBF in the PCC was probably caused by the abnormal pathology in the entorhinal cortex. In addition, atrophy in the entorhinal cortex on MRI [18] and reduction of rCBF in the PCC and precuneus on SPECT [19] predict progression from MCI to AD. We used two reliable and user-independent statistical image-analyzing methods, VSRAD and 3D-SSP, to detect AD-specific abnormalities in the MR and SPECT images.

This is the first report to compare cognitive impairment between ES and AD-aMCI. The WMS-R GM indices of the two groups were comparable, indicating a similarity in the impairment of recent memory between the two groups. Some previous studies compared recent memory in ES and AD at the dementia stage. There is some disagreement on whether recent memory is better [20] or worse [21] in ES than in AD in the dementia stage. aMCI is a relatively homogeneous group with respect to memory impairment, because the definition of aMCI includes the degree of memory impairment. However, the severity of recent memory impairment could vary in patients with ES. The ES patients in this study were mild cases, because they could complete the WMS-R or WAIS-R, which are comprehensive tests, and the mean duration of their hospitalization was short. Thus, the recent memory tests in this study indicated that the recent memory scores of ES patients with mild cognitive impairment were comparable with those of AD-aMCI patients, and, therefore, that recent memory was not useful for distinguishing between ES and AD-aMCI.

The fact that the WMS-R GM indices were comparable in the ES and AD-aMCI groups indicates that the two groups in this study had similar degrees of impairment of recent memory. This narrows down the difference between the two groups to differences in other cognitive impairments, such as forgetfulness, and impairments of DR, attention, working memory and executive function. The WMS-R GM-DR scores were lower and the DR scores were higher in ES than in AD-aMCI, indicating that the degree of forgetfulness was less and DR was better in ES. On the other hand, the AC was lower in ES than in AD-aMCI, indicating that ES patients had more impaired attention and working memory than AD-aMCI patients. DR was found to be better in ES patients than in AD patients in the dementia stage [21], and forgetfulness did not increase in ES patients but increased in AD patients in the dementia stage [20]. The present study confirmed that memory after a short while was retained in ES but not in AD. In addition, we found that the retention in ES patients was better than in AD even at the aMCI stage, which should help to distinguish ES from AD in the very early stage.

The hippocampus, parahippocampus, and entorhinal cortex have traditionally been thought of as the principal structures responsible for the consolidation of short-term stores into long-term memory. Significant associations between hippocampal size and memory have not been observed in schizophrenia [22], although size reductions in the hippocampus have been reported in schizophrenia [2]. In addition, memory capabilities were similar to general intellectual abilities in ES [23]. Therefore, damage in the medial temporal lobe may not play an important role in memory impairment in schizophrenia. On the other hand, memory impairment in AD is inversely associated with hippocampal volume [24].

The ES group was more impaired on the digit symbol substitution, similarities, picture completion, and block design subtests of WAIS-R than the AD-aMCI group, and each subtest score in the ES group was below the mean of each score of the general population in this study. Although the block design subtest was used to evaluate visuoconstructive function in

Dement Geriatr Cogn Disord Extra 2011;1:20–30
DOI: 10.1159/000323561
Published online: January 6, 2011

this study, attention and executive function are required to perform the block design subtest [25]. Thus, these findings confirmed that attention, working memory, and executive function are impaired in ES. Previous studies reported that ES patients were impaired in the WAIS-R digit symbol substitution, similarities, picture completion, and block design subtests [21], and in attention, working memory, and executive function [20]. These studies also reported that impairment in these functions were comparable in ES and AD patients in the dementia stage. The differences in cognitive impairment that we found in ES and AD-aMCI deviate from those found in previous studies. This discrepancy may be due to differences in the severity of cognitive impairments in the AD-aMCI patients in this study compared to the AD patients in the dementia stage in previous studies.

Which region of the brain is responsible for the difference in attention, working memory, and executive function in the two groups? Impairments in cognitive function in patients with schizophrenia were found to be related to dysfunction of the prefrontal cortex (PFC) [26]. On the other hand, gray matter loss on MRI [27] and pathological abnormality [28] in the PFC were not observed in AD-aMCI, and gray matter loss on MRI was observed at the time of progression from aMCI to AD [27]. These results suggest that differences in impairment in attention, working memory, and executive function in the two groups probably reflect the difference in impairment in the PFC.

The WAIS-R information scores of the ES and AD-aMCI groups were comparable and within the normal range, being consistent with those of a previous study [29]. Semantic memory may be preserved in ES and AD-aMCI patients because they have less impairment in the inferior and anterior temporal lobe regions, which crucially contribute to semantic cognition [30].

There were some limitations in this study. First, approximately half of the patients in each group were not given the WAIS-R. Second, the ES patients in this study were younger than the AD-aMCI patients, and cognitive function in schizophrenia patients undergoes a marked decline after 65 years of age [8]. Third, we did not control the effects of medication on the cognitive test scores in ES patients. Most ES subjects in this study had received atypical antipsychotic drugs, which might improve cognitive function [31]. These issues should be taken into consideration before the findings are generalized.

In this study, DR and forgetfulness were less impaired in ES than in AD-aMCI, while attention, working memory, and executive function were more impaired in ES than in AD-aMCI. The results of this study should help clinicians to distinguish patients with ES from patients with AD-aMCI and might also give us some clues for distinguishing ES combined with AD-aMCI from ES alone. The next step is to clarify the difference in the characteristics of cognitive impairment in ES combined with AD-aMCI compared to ES alone.

Acknowledgments

Funding for this study was provided by Research Grants for Research on Dementia (H21-Dementia-General-003 and H22-Dementia-General-003) and Grants-in-Aid (H19-kokoro-002) from the Japanese Ministry of Health, Labor and Welfare, and by the Japanese Ministry of Education, Culture, Sports, Science and Technology (17191211, 18689030, 18023045, 20591402, and 21591514).

Disclosure Statement

The authors declare that they have no conflict of interest.

Dement Geriatr Cogn Disord Extra 2011;1:20–30
DOI: 10.1159/000323561
Published online: January 6, 2011

References

1 Van Os J, Kapur S: Schizophrenia. Lancet 2009;374:635–645.
2 Hirayasu Y, Shenton ME, Salisbury DF, Dickey CC, Fischer IA, Mazzoni P, Kisler T, Arakaki H, Kwon JS, Anderson JE, Yurgelun-Todd D, Tohen M, McCarley RW: Lower left temporal lobe MRI volumes in patients with first-episode schizophrenia compared with psychotic patients with first-episode affective disorder and normal subjects. Am J Psychiatry 1998;155:1384–1391.
3 Goldman AL, Pezawas L, Mattay VS, Fischl B, Verchinski BA, Chen Q, Weinberger DR, Meyer-Lindenberg A: Widespread reductions of cortical thickness in schizophrenia and spectrum disorders and evidence of heritability. Arch Gen Psychiatry 2009;66:467–477.
4 Laakso MP, Soininen H, Partanen K, Helkala EL, Hartikainen P, Vainio P, Hallikainen M, Hanninen T, Riekkinen PJ Sr: Volumes of hippocampus, amygdala and frontal lobes in the MRI-based diagnosis of early Alzheimer's disease: correlation with memory functions. J Neural Transm Park Dis Dement Sect 1995;9:73–86.
5 Dickinson D, Ramsey ME, Gold JM: Overlooking the obvious: a meta-analytic comparison of digit symbol coding tasks and other cognitive measures in schizophrenia. Arch Gen Psychiatry 2007;64:532–542.
6 Winblad B, Wimo A, Engedal K, Soininen H, Verhey F, Waldemar G, Wetterholm AL, Haglund A, Zhang R, Schindler R: 3-year study of donepezil therapy in Alzheimer's disease: effects of early and continuous therapy. Dement Geriatr Cogn Disord 2006;21:353–363.
7 Petersen RC, Smith GE, Waring SC, Ivnik RJ, Tangalos EG, Kokmen E: Mild cognitive impairment: clinical characterization and outcome. Arch Neurol 1999;56:303–308.
8 Friedman JI, Harvey PD, Coleman T, Moriarty PJ, Bowie C, Parrella M, White L, Adler D, Davis KL: Six-year follow-up study of cognitive and functional status across the lifespan in schizophrenia: a comparison with Alzheimer's disease and normal aging. Am J Psychiatry 2001;158:1441–1448.
9 Lawton MP, Brody EM: Assessment of older people: self-maintaining and instrumental activities of daily living. Gerontologist 1969;9:179–186.
10 Hirata Y, Matsuda H, Nemoto K, Ohnishi T, Hirao K, Yamashita F, Asada T, Iwabuchi S, Samejima H: Voxel-based morphometry to discriminate early Alzheimer's disease from controls. Neurosci Lett 2005;382:269–274.
11 Minoshima S, Berger KL, Lee KS, Mintun MA: An automated method for rotational correction and centering of three-dimensional functional brain images. J Nucl Med 1992;33:1579–1585.
12 Mizumura S, Kumita S, Cho K, Ishihara M, Nakajo H, Toba M, Kumazaki T: Development of quantitative analysis method for stereotactic brain image: assessment of reduced accumulation in extent and severity using anatomical segmentation. Ann Nucl Med 2003;17:289–295.
13 Kazui H, Ishii R, Yoshida T, Ikezawa K, Takaya M, Tokunaga H, Tanaka T, Takeda M: Neuroimaging studies in patients with Charles Bonnet syndrome. Psychogeriatrics 2009;9:77–84.
14 Misawa Y: Manual of the Short Form of the Japanese Version of the WAIS-R (in Japanese). Tokyo, Nihon Bunka Kagakusha, 1993.
15 Gomez-Isla T, Price JL, McKeel DW Jr, Morris JC, Growdon JH, Hyman BT: Profound loss of layer II entorhinal cortex neurons occurs in very mild Alzheimer's disease. J Neurosci 1996;16:4491–4500.
16 Killiany RJ, Gomez-Isla T, Moss M, Kikinis R, Sandor T, Jolesz F, Tanzi R, Jones K, Hyman BT, Albert MS: Use of structural magnetic resonance imaging to predict who will get Alzheimer's disease. Ann Neurol 2000;47:430–439.
17 Mosconi L, Pupi A, De Cristofaro MT, Fayyaz M, Sorbi S, Herholz K: Functional interactions of the entorhinal cortex: an 18F-FDG PET study on normal aging and Alzheimer's disease. J Nucl Med 2004;45:382–392.
18 Killiany RJ, Hyman BT, Gomez-Isla T, Moss MB, Kikinis R, Jolesz F, Tanzi R, Jones K, Albert MS: MRI measures of entorhinal cortex vs hippocampus in preclinical AD. Neurology 2002;58:1188–1196.
19 Kogure D, Matsuda H, Ohnishi T, Asada T, Uno M, Kunihiro T, Nakano S, Takasaki M: Longitudinal evaluation of early Alzheimer's disease using brain perfusion SPECT. J Nucl Med 2000;41:1155–1162.
20 Heaton R, Paulsen JS, McAdams LA, Kuck J, Zisook S, Braff D, Harris J, Jeste DV: Neuropsychological deficits in schizophrenics. Relationship to age, chronicity, and dementia. Arch Gen Psychiatry 1994;51:469–476.

Dement Geriatr Cogn Disord Extra 2011;1:20–30
DOI: 10.1159/000323561
Published online: January 6, 2011

www.karger.com/dee

21 Zakzanis KK, Andrikopoulos J, Young DA, Campbell Z, Sethian T: Neuropsychological differentiation of late-onset schizophrenia and dementia of the Alzheimer's type. Appl Neuropsychol 2003;10:105–114.
22 Torres IJ, Flashman LA, O'Leary DS, Swayze V 2nd, Andreasen NC: Lack of an association between delayed memory and hippocampal and temporal lobe size in patients with schizophrenia and healthy controls. Biol Psychiatry 1997;42:1087–1096.
23 Hawkins KA: Memory deficits in patients with schizophrenia: preliminary data from the Wechsler Memory Scale-Third Edition support earlier findings. J Psychiatry Neurosci 1999;24:341–347.
24 Mori E, Yoneda Y, Yamashita H, Hirono N, Ikeda M, Yamadori A: Medial temporal structures relate to memory impairment in Alzheimer's disease: an MRI volumetric study. J Neurol Neurosurg Psychiatry 1997;63:214–221.
25 Chase TN, Fedio P, Foster NL, Brooks R, Di Chiro G, Mansi L: Wechsler Adult Intelligence Scale performance. Cortical localization by fluorodeoxyglucose F18-positron emission tomography. Arch Neurol 1984;41:1244–1247.
26 Ikezawa K, Iwase M, Ishii R, Azechi M, Canuet L, Ohi K, Yasuda Y, Iike N, Kurimoto R, Takahashi H, Nakahachi T, Sekiyama R, Yoshida T, Kazui H, Hashimoto R, Takeda M: Impaired regional hemodynamic response in schizophrenia during multiple prefrontal activation tasks: a two-channel near-infrared spectroscopy study. Schizophr Res 2009;108:93–103.
27 Whitwell JL, Przybelski SA, Weigand SD, Knopman DS, Boeve BF, Petersen RC, Jack CR Jr: 3D maps from multiple MRI illustrate changing atrophy patterns as subjects progress from mild cognitive impairment to Alzheimer's disease. Brain 2007;130:1777–1786.
28 Petersen RC, Parisi JE, Dickson DW, Johnson KA, Knopman DS, Boeve BF, Jicha GA, Ivnik RJ, Smith GE, Tangalos EG, Braak H, Kokmen E: Neuropathologic features of amnestic mild cognitive impairment. Arch Neurol 2006;63:665–672.
29 Kirkpatrick B, Messias E, Harvey PD, Fernandez-Egea E, Bowie CR: Is schizophrenia a syndrome of accelerated aging? Schizophr Bull 2008;34:1024–1032.
30 Visser M, Embleton KV, Jefferies E, Parker GJ, Ralph MA: The inferior, anterior temporal lobes and semantic memory clarified: novel evidence from distortion-corrected FMRI. Neuropsychologia 2010;48:1689–1696.
31 Houthoofd SA, Morrens M, Sabbe BG: Cognitive and psychomotor effects of risperidone in schizophrenia and schizoaffective disorder. Clin Ther 2008;30:1565–1589.

JBC Papers in Press. Published on March 7, 2012 as Manuscript M111.325456
The latest version is at http://www.jbc.org/cgi/doi/10.1074/jbc.M111.325456

Phenolic Compounds Prevent Amyloid β-Protein Oligomerization and Synaptic Dysfunction by Site Specific Binding*

Kenjiro Ono[1], Lei Li[2], Yusaku Takamura[3], Yuji Yoshiike[4], Lijun Zhu[2], Fang Han[2], Xian Mao[2], Tokuhei Ikeda[1], Jun-ichi Takasaki[1], Hisao Nishijo[3], Akihiko Takashima[4], David B. Teplow[5], Michael G. Zagorski[2], and Masahito Yamada[1]

[1]Department of Neurology and Neurobiology and Aging, Kanazawa University Graduate School of Medical Science, Kanazawa 920-8640, Japan, [2]Department of Chemistry, Case Western Reserve University, Cleveland, OH 44106 USA, [3]System Emotional Science, University of Toyama, Toyama 930-0194, Japan, [4]Laboratory for Alzheimer's Disease, Brain Science Institute, Riken, 2-1 Hirosawa, Wako, Saitama 351-0198, Japan and [5]Department of Neurology and Mary S. Easton Center for Alzheimer's Disease Research at UCLA, David Geffen School of Medicine, and Molecular Biology Institute and Brain Research Institute, University of California, Los Angeles, CA 90095 USA

*Running title: Phenolic Compounds Prevent Aβ Oligomerization

*To whom correspondence should be addressed to Michael G. Zagorski, Department of Chemistry, Case Western Reserve University, Cleveland, OH 44106 USA, Tel.: +1- 216-368-3706;Fax: +1- 216-368-3006 E-mail: michael.zagorski@case.edu or Masahito Yamada, Department of Neurology and Neurobiology of Aging, Kanazawa University Graduate School of Medical Science, Kanazawa 920-8640, Japan, Tel.: +81-76-265-2290; Fax: +81-76-234-4253; E-mail: m-yamada@med.kanazawa-u.ac.jp

Key words: amyloid β-protein, Alzheimer's disease, phenolic compounds, oligomer, synaptic toxicity

CAPSULE

Background: Epidemiological evidence suggests that consumption of phenolic compounds reduce the incidence of Alzheimer's disease (AD).

Results: Myricetin and rosmarinic acid reduced cellular and synaptic toxicities by inhibition of amyloid β-protein (Aβ) oligomerization. Myricetin promoted NMR changes of Aβ.

Conclusion: Phenolic compounds are worthy therapeutic candidates for AD.

Significance: Phenolic compounds blocked early assembly processes of Aβ through differently binding.

SUMMARY

Cerebral deposition of amyloid β-protein (Aβ) is an invariant feature of Alzheimer's disease (AD), and epidemiological evidence suggests that moderate consumption of foods enriched with phenolic compounds reduce the incidence of AD. We previously reported that the phenolic compounds myricetin (Myr) and rosmarinic acid (RA) inhibited Aβ aggregation *in vitro* and *in vivo*. To elucidate a mechanistic basis for these results, we analyzed the effects of five phenolic compounds in the Aβ aggregation process and in oligomer-induced synaptic toxicities. We now report that the phenolic compounds blocked Aβ oligomerization, and Myr promoted significant NMR chemical shift changes of monomeric Aβ. Both Myr and RA reduced cellular toxicity and synaptic dysfunction of the Aβ oligomers. These results suggest that Myr and RA may play key roles in blocking the toxicity and early assembly processes associated with Aβ through differently binding.

Alzheimer's disease (AD) has been characterized historically by the accumulation of intraneuronal filaments formed by the microtubule-associated protein tau and of extracellular parenchymal and vascular amyloid deposits largely comprising the amyloid β-protein (Aβ) (1). Continuing investigations of

the pathogenetic relationships among tau, Aβ, and AD suggest that oligomeric forms of Aβ play a seminal role in disease causation (1,2). More recent evidence suggests that low n-order oligomers are especially important (3). Townsend *et al.* found that Aβ trimers fully inhibit long-term potentiation, whereas dimers and tetramers have an intermediate potency (4). Dimers and trimers from the conditioned medium of amyloid precursor protein (APP)-expressing CHO cells have been found to cause progressive loss of synapses in organotypic rat hippocampal slices (5). Aβ oligomers extracted from AD brains disrupt synaptic function, and dimers were the smallest oligomers showing activity (6). Recently, structure–cytotoxicity studies of pure Aβ oligomer populations produced the first determinations of oligomer specific activity (7), in that dimers, trimers, and tetramers all were significantly more toxic than monomers. Importantly, a non-linear dependence of cytotoxicity on oligomer order was observed. Thus, the most efficacious therapeutic agents should perhaps target monomeric Aβ and prevent its assembly into any sized oligomer (3).

Nature itself may have created useful therapeutic agents of AD. The relevance of this finding to AD has come from French and Danish epidemiological studies suggesting that moderate wine drinking may protect against AD (8,9). Investigation of this phenomenon may reveal the answer for wine's protective effects against AD. Classical biochemical fractionation studies have shown that the active components of red wine are phenolic compounds, including resveratrol and the proanthocyanidins (10). Resveratrol was found to lower significantly the levels of secreted and intracellular Aβ produced in a variety of cell lines by increasing proteasome-mediated Aβ degradation (11). Interestingly, a related polyphenolic compound, curcumin (Cur), is found in the common spice curry (12). As with red wine, epidemiologic studies have shown a correlation between curry consumption and decreased AD risk (13). The concordance of results from these different systems emphasizes the potential importance of elucidating the mechanism through which phenolic compounds may alter Aβ aggregation and toxicity.

Initial mechanistic studies have focused on formation of large aggregates, Aβ fibrils (fAβ). Phenolic compounds, such as the wine related polyphenol myricetin (Myr), a major component of curry spice turmeric Cur, its analog rosmarinic acid (RA), nordihydroguaiaretic acid (NDGA), and ferulic acid (FA) inhibit the formation of fAβ as well as dissociate preformed fibrils by preferentially and reversibly binding to these structures (14-16). In cell culture experiments, Myr-treated fAβ were less toxic than intact fAβ (14). Recently, a commercially available grape seed polyphenolic extract, MegaNatural®, was shown to inhibit significantly the aggregation of Aβ into sodium dodecyl sulfate (SDS)-stable high molecular weight (HMW) oligomers (15-20 monomers) using AD model transgenic animals (Tg2576)(17). We showed that the phenolic compounds such as Myr, Cur, and RA prevented the development of AD pathology and reduced HMW oligomers in Tg2576 mice (18).

In the studies reported here, we sought to determine how the phenolic compounds affected Aβ conformational dynamics and the early stages of Aβ assembly. To do so, we analyzed the assembly of the Aβ42 and Aβ40 with five phenolic compounds, Myr, FA, NDGA, Cur, and RA (**Fig. 1**) using several well-established techniques for studying amyloid formation, including photo-induced cross-linking of unmodified proteins (PICUP), atomic force microscopy (AFM), circular dichroism spectroscopy (CD), and nuclear magnetic resonance (NMR). Next, we examined whether the phenolic compounds reduced Aβ assembly-induced cytotoxicity and synaptic dysfunction using 3-(19)-2,5-diphenyltetrazolium bromide (MTT) assays and electrophysiological assays for long-term potentiation (LTP) and depression (LTD) in hippocampal slices.

EXPERIMENTAL PROCEDURES

Chemicals and reagents - Chemicals were obtained from Sigma-Aldrich Co. (St. Louis, MO) and were of the highest purity available. Water was produced using a Milli-Q system (Nihon Millipore K.K., Japan).

Proteins and phenolic compounds - Aβ peptides were synthesized, purified, and characterized as described previously (20,21). Briefly, synthesis was performed on an automated peptide synthesizer (Model 433A, Applied Biosystems, CA) using 9-fluorenylmethoxycarbonyl-based methods on pre-loaded Wang resins. Peptides were purified using reverse-phase high-performance liquid chromatography (RP-HPLC). Quantitative amino acid analysis and mass spectrometry yielded the expected compositions and molecular weights, respectively, for each peptide. Purified peptides were stored as lyophilizates at –20°C. [Met(O)^{35}]Aβ42 peptide was purchased from Bachem AG (Bubendorf, Switzerland). To prepare peptides for study, Aβ peptide lyophilizates were dissolved at a nominal concentration of 25 or 50 μM in 10% (v/v) 60 mM NaOH and 90% (v/v) 10 mM phosphate buffer, pH 7.4. After sonication for 1 min, the peptide solution was centrifuged for 10 min at 16,000 x *g*. A stock solution of GST (Sigma-Aldrich, St. Louis, MO) was prepared by dissolving the lyophilizate to a concentration of 250 μM in 60 mM NaOH. Prior to use, aliquots were diluted 10-fold into 10 mM sodium phosphate, pH 7.4. We examined 5-phenolic compounds such as Myr, FA, NDGA, Cur, and RA. They were dissolved in ethanol to a final concentration of 2.5 mM and then diluted with 10 mM phosphate, pH 7.4, to produce concentrations of 5, 10, 25, 50, 100, and 500 μM for CD, PICUP, and AFM, as described previously (20).

CD - CD spectra of Aβ:compound mixtures were acquired immediately after sample preparation or following 2, 3, 5, or 6 days of incubation. CD measurements were made by removing a 200 μl aliquot from the reaction mixture, adding the aliquot to a 1 mm path length CD cuvette (Hellma, Forest Hills, NY), and acquiring spectra in a J-805 spectropolarimeter (JASCO, Japan). The CD cuvettes were maintained on ice prior to introduction into the spectrometer. Following temperature equilibration, spectra were recorded at 22°C from ~190-260 nm at 0.2 nm resolution with a scan rate of 100 nm/min. Ten scans were acquired and averaged for each sample. Raw data were manipulated by smoothing and subtraction of buffer spectra according to the manufacturer's instructions.

Chemical cross-linking and determination of oligomer frequency distributions - Immediately after their preparation, samples were cross-linked using PICUP, as described (22). Briefly, to 18 μl of 50 μM protein solution were added 1 μl of 4 mM tris(2,2'-bipyridyl)dichlororuthenium(II) (Ru(bpy)) and 1 μl of 80 mM ammonium persulfate (APS). The final protein:Ru(bpy):APS molar ratios of Aβ40 or Aβ42 was 1:4:80. The mixture was irradiated for 1 sec with visible light and then the reaction was quenched with 2 μl of 1 M dithiothreitol (DTT) (Invitrogen, CA) in ultrapure water. Determination of the frequency distribution of monomers and oligomers was accomplished using SDS-polyacrylamide gel electrophoresis (SDS-PAGE) and silver staining, as described (22). Briefly, 8 μl of each cross-linked sample was electrophoresed on a 10-20% gradient tricine gel and visualized by silver staining (Invitrogen). Uncross-linked samples were used as controls in each experiment. Densitometry was performed with a luminescent image analyzer (LAS 4000 mini, Fujifilm, Tokyo) and image analysis software (Multi gauge v. 3.2., Fujifilm). The intensity of each band in a lane from the SDS gel was normalized to the sum of the intensities of all the bands in that lane, according to the formula $R_i = I_i \Big/ \sum_{i=1}^{n} I_i$ x 100 (%), where R_i is the normalized intensity of band I and I_i is the intensity of each band i. R_i varies from 0–100. To calculate the oligomers ratio, the sum of oligomers intensities of Aβ40 or Aβ42 with 5, 10, 25, 50, 100, and 500 μM Myr, FA, NDGA, Cur or RA was divided by the sum of oligomers intensities without each compound. The EC_{50} was defined as the concentration of Mel to inhibit αS oligomerization to 50% of the control value. EC_{50} was calculated by sigmoidal curve fitting, using GraphPad Prism software (version 4.0a, GraphPad Software, Inc., CA).

Size-exclusion chromatography (SEC) - PICUP

reagents and phenolic compounds were removed from cross-linked samples by SEC as described previously(23). To do so, 1.5 cm diameter cylindrical columns were packed manually with 2 g of Bio-Gel P2 Fine (Bio-Rad Laboratories, CA), which produced a 6 ml column volume. The column first was washed twice with 25 ml of 50 mM NH_4HCO_3, pH 8.5. Two-hundred sixteen µl of cross-linked sample then was loaded. The column was eluted with the same buffer at a flow rate of ≈ 0.15 ml/min. The first 1 ml of eluate was collected. The fractionation range of the Bio-Gel P2 column is 100-1800 Da. Aβ peptides thus elute in the void volume whereas Ru(bpy) (MW=748.6), APS (MW=228.2), Myr (MW=318.2), RA (MW=360.3), and DTT (MW=154.2) enter the column matrix and are separated from Aβ.

Fractions were lyophilized immediately after collection. Reconstitution of the lyophilizates to a nominal concentration of 25 µM in 10 mM sodium phosphate, pH 7.4, followed by the SDS-PAGE analysis, showed that removal of reagents and phenolic compounds, lyophilization, and reconstitution did not alter the oligomer composition of any of the peptide populations under study (**Fig. S1**).

AFM - Peptide solutions were characterized using a Nanoscope IIIa controller (Veeco Digital Instruments, CA) with a multimode scanning probe microscope equipped with a JV scanner. All measurements were carried out in the tapping mode under ambient conditions using single-beam silicon cantilever probes. A 10 µl aliquot of each peptide lyophilizate, reconstituted to a concentration of 25 µM in 10 mM PBS, pH 7.4, was spotted onto freshly cleaved mica (Ted Pella, Inc., CA), incubated at room temperature for 5 min, rinsed with water, and then blown dry with air. At least four regions of the mica surface were examined to confirm the homogeneity of the structures throughout the sample. Mean particle heights were analyzed by averaging the measures values of eight individual cross-sectional line scans from each image only when the particle structure was confirmed.

NMR spectroscopy - Stock solutions of the five phenolic compounds (2.5 mM), and monomeric, uniformly ^{15}N-labelled Aβ42 peptide (0.25 mM) (rPeptide, GA) and Aβ40 (0.25 mM) were prepared by dissolution (with sonication) in aqueous basic solution (pD 11, 1 ml, 10 mM NaOD) (21). Aliquots of the Aβ42 and phenolic solutions were combined and mixed with cold (5°C) phosphate buffer solution (0.5-1.0 ml, 5 mM, pH 7.5) that contained 0.5 mM predeuterated ethylenediamine tetraacetic acid (Na_2EDTA-d_{12}), and 0.05 mM NaN_3. The aliquots were varied so that the final peptide:compound concentration ratio was 25 µM : 500 µM. To prevent aggregation, peptide solutions were kept cold (5°C) and standard ^1H-^{15}N HSQC spectra were obtained within 30-min of the sample preparation. Spectra were obtained at 5°C with a Bruker Avance-II 900 MHz spectrometer equipped with a TXI cryoprobe (Bruker BioSpin, Inc., CA).

The saturation transfer difference (STD) experiments were obtained with the Aβ40 (25 µM) alone or with RA or Myr (50 µM) at pH 7.5 and 5°C. Data was acquired at 900.18 MHz using the pulse program (selective irradiation)-(non selective excitation)-(watergate)-(acquisition) (24,25). The selective irradiation used a 3.9-s long and weak pulse that was alternatively applied at -0.2 ppm (where there was a peak) and at 30 ppm (where there was no peak), the latter constituting the reference spectra. The non-selective excitation was achieved with a 90° pulse at the water position (4.7 ppm), and the Watergate 3-9-19 pulse sequence was used to suppress the water signal. Each spectrum was acquired with 128-scans (12-min), and stored separately. The STD was obtained by subtracting the reference spectra from that obtained with irradiation at -0.2 ppm.

All NMR spectra were processed with the NMRPipe (26), Mnova (http://mestrelab.com/software/mnova-nmr/), or CARA (http://cara.nmr.ch) programs using a PC computer.

NMR-based molecular modeling - Atomic coordinates of the NMR/molecular dynamics Aβ42 structural model were kindly provided by Dr. Chunyu Wang (Rensselaer Polytechnic Institute, NY) (27). With the model, the regions